Quantum phase communication channels in the presence of static and dynamical phase diffusion

Jacopo Trapani,[1,*] Berihu Teklu,[2,†] Stefano Olivares,[1,3,4,‡] and Matteo G. A. Paris[1,3,4,§]
[1]*Dipartimento di Fisica, Università degli Studi di Milano, I-20133 Milano, Italy*
[2]*Institut Pascal, PHOTON-N2, Clermont Université, Blaise Pascal University, CNRS, F-63177 Aubière Cedex, France*
[3]*CNISM, UdR Milano Statale, I-20133 Milano, Italy*
[4]*INFN, Sezione di Milano, I-20133 Milano, Italy*
(Received 12 May 2015; published 15 July 2015)

We address quantum communication channels based on phase modulation of coherent states and analyze in detail the effects of static and dynamical (stochastic) phase diffusion. We evaluate mutual information for an ideal phase receiver and for a covariant phase-space-based receiver, and compare their performances by varying the number of symbols in the alphabet and/or the overall energy of the channel. Our results show that phase communication channels are generally robust against phase noise, especially for large alphabets in the low-energy regime. In the presence of dynamical (non-Markovian) noise the mutual information is preserved by the time correlation of the environment, and when the noise spectra are detuned with respect to the information carrier, revivals of mutual information appear.

DOI: 10.1103/PhysRevA.92.012317 PACS number(s): 03.67.Hk, 03.65.Wj, 03.65.Ta

I. INTRODUCTION

The transmission of classical information along an ideal bosonic quantum channel is optimized by encoding information onto Fock number states, according to a thermal distribution, and then retrieving this information by the measurement of the number of photons [1–3]. This strategy allows us to achieve the ultimate channel capacity, i.e., to maximize the mutual information between the sender and the receiver, given a constraint on the overall energy sent through the channel, thus outperforming other encoding-decoding schemes involving different degrees of freedom of the radiation field, e.g., the amplitude or the phase.

If we take into account the unavoidable noise affecting the information carriers along the channel, the situation becomes more involved and a question arises on whether different encoding-decoding schemes may offer better or comparable performances. Indeed, in the presence of a phase-insensitive noise, e.g., amplitude damping, also coherent coding has been shown to achieve the ultimate channel capacity [4,5].

In this paper, we address communication channels based on phase encoding [6–8] and analyze in detail their performances in the presence of phase diffusion, which represents the most detrimental kind of noise affecting this kind of channel [9,10]. In particular, we will consider communication schemes where the information is encoded by modulating the phase of a coherent signal, which then travels through a phase-diffusing environment before arriving at the receiver station and being detected. We consider two different environment models in which phase noise is either induced by a stationary environment inducing a static noise, or by a fluctuating one leading to stochastic phase diffusion. We then evaluate the mutual information for both an ideal phase receiver and a covariant phase-space-based one (corresponding to the marginal phase distribution of the Husimi Q function). We then compare their performances to each other and with the capacity of other relevant channels, including the optimal one. Our results show that phase-keyed communication channels are robust against phase diffusion and offer performances comparable to channels involving coherent encoding. Phase channels may even approach the ultimate capacity in the low-energy regime and for large alphabets.

The paper is structured as follows. In Sec. II we describe the communication protocol details and derive a general formula for the corresponding mutual information. In Sec. III we introduce a model for the static noise case and discuss the effects on the channel performance, making a comparison with the cases of photon number and amplitude channels. Section IV considers channels affected by dynamical (stochastic) phase diffusion and discusses the significative differences with the static case. Section V closes the paper with some concluding remarks.

II. PHASE-KEYED COMMUNICATION CHANNELS

A schematic diagram of a quantum phase communication channel is depicted in Fig. 1. The sender encodes a finite number N of symbols using N different values of a phase shift ϕ_k, where $\phi_k < \phi_j$ if $k < j$ and $0 \leqslant k < N$. We assume a choice of equidistant phase values $\phi_k = 2\pi k/N$. The phase ϕ_k is encoded onto a *seed* state ρ_0 of a single-mode radiation field by the unitary phase-shift operation $U(\phi) = \exp(i\phi\, a^\dagger a)$, a being the annihilation operator, $[a, a^\dagger] = 1$; namely,

$$\rho_0 \to \rho_k \equiv U(\phi_k)\rho_0 U^\dagger(\phi_k). \tag{1}$$

The signal then propagates along the channel to the receiver station, where it is detected by a suitable measurement scheme in order to retrieve the information it carries. More explicitly, the receiver performs a phase measurement on the output state and, once the phase is measured, she chooses a strategy to associate the measured value to one of the symbols of the sender's alphabet. The inference strategy should match the (continuous) output from the phase measurement to a symbol from a discrete alphabet. The straightforward choice consists

*jacopo.trapani@unimi.it
†berihut@gmail.com
‡stefano.olivares@fisica.unimi.it
§matteo.paris@fisica.unimi.it

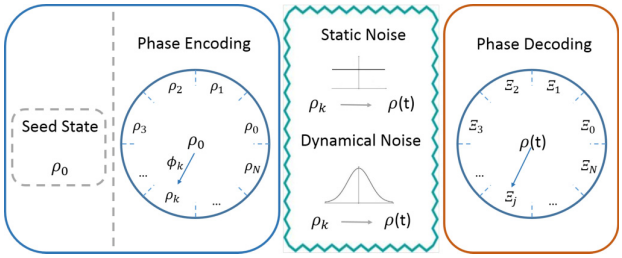

FIG. 1. (Color online) Schematic representation of a phase communication channel. The sender encodes a finite number N of symbols using N different values of a phase shift $\phi_k = 2\pi k/N$ imposed on a *seed* coherent state ρ_0. The signal then propagates along the channel, to the receiver station, in the presence of either static or dynamical noise, and it is finally detected by a suitable measurement scheme in order to retrieve the carried information.

of associating each phase value with the closest ϕ_k within a margin of error. To this aim the receiver divides the full phase range $[0,2\pi)$ into N bins, corresponding to the intervals

$$\Xi_j = [\phi_j - \Delta, \phi_j + \Delta),$$

where $\Delta = \pi/N$ and $\bigcup_{j=1}^{N} \Xi_j = [0,2\pi)$. More generally, the width of each bin may be different and dependent on j, though a symmetric choice is often optimal and will be assumed throughout this paper. If ϕ denotes the value of the receiver's outcome, we express the inference rule as follows:

$$\text{if} \quad \phi \in \Xi_j \Rightarrow \quad \phi \to \phi_j. \tag{2}$$

The positive operator-valued measure (POVM) $\{\Pi(\phi_j)\} \equiv \{\Pi_j\}$ describing the measurement strategy employed by the receiver can be written as

$$\Pi_j = \int_{\phi_j - \Delta}^{\phi_j + \Delta} \pi(\theta) d\theta, \tag{3}$$

where $\pi(\theta)$ is the actual POVM of the phase measurement performed by the receiver. A POVM for a covariant phase measurement may always be written as [12,13]

$$\pi(\theta) = \frac{1}{2\pi} \sum_{n,m=0}^{\infty} A_{n,m} e^{-i(n-m)\theta} |n\rangle\langle m|, \tag{4}$$

where $A_{n,m}$ are the elements of a positive and Hermitian matrix $\boldsymbol{A}$, which is measurement-dependent. Covariance follows easily from Eq. (4), since $U(\phi)\pi(\theta)U^{\dagger}(\phi) = \pi(\theta + \phi)$ and thus

$$\Pi_j = U(\phi_j)\Pi_0 U^{\dagger}(\phi_j). \tag{5}$$

The combination of Eqs. (3) and (4) brings to an explicit form of the POVM Π_j, given by

$$\Pi_j = \sum_{n,m=0}^{\infty} A_{n,m} f_{n-m}(j) |n\rangle\langle m|, \tag{6}$$

where the structure of the POVM is determined by the resolution function

$$f_d(j) = \frac{1}{2\pi} \int_{\phi_j - \Delta}^{\phi_j + \Delta} e^{-id\theta} d\theta = \frac{\sin \Delta\pi}{\pi d} e^{-id\phi_j}, \tag{7}$$

with the property $\sum_{j=1}^{N} f_d(j) = \delta_{d,0}$, where δ is the Kronecker delta.

The figure of merit to assess the performances of a communication channel is the mutual information between sender and receiver. This quantity measures the amount of information shared by the two parties and can be written as

$$\begin{aligned} I &= \sum_{k,j=0}^{N-1} p(k,j) \log_2 \frac{p(k,j)}{p(k)\, p'(j)} \\ &= \sum_{k,j=0}^{N-1} p(j|k) p(k) \log_2 \frac{p(j|k)}{p'(j)}, \end{aligned} \tag{8}$$

where $p(k)$ is the *a priori* probability distribution of transmitting a ϕ_k-encoded seed state; $p(k,j) = p(j|k)\, p(k)$ is the joint probability to send the symbol ϕ_k and obtaining the outcome ϕ_j; $p'(j) \equiv p'(\phi_j)$ is the probability of the outcome ϕ_j, given by $p'(j) = \sum_{k=0}^{N-1} p(j|k)p(k)$; and, finally, $p(j|k)$ is the conditional probability of measuring a phase ϕ_j given the input phase ϕ_k or, in other words, the conditional probability of an outcome ϕ falling in the bin Ξ_j given the initial state ρ_k, which is given by

$$p(\phi \in \Xi_j | \rho_k) \equiv p(j|k) = \mathrm{Tr}[\rho_k \Pi_j]. \tag{9}$$

Maximization over the *a priori* probability $p(\phi_k)$ leads to the so called channel capacity, i.e., the maximum information transmitted through the channel per use. In our case, this is achieved using a uniform encoding probability, $p(k) = N^{-1}$; i.e., the letters have the same probability to be sent through the channel. The proof follows from the covariance of the receiver's POVM in Eq. (5) together with the convexity of the Shannon entropy and with the fact that phase noise, as we will see in the following, commutes with the encoding procedure in Eq. (1). As a consequence, the mutual information given in Eq. (8) is the *channel capacity* of the phase-keyed communication channel, and may be rewritten as

$$I = \frac{1}{N} \sum_{k,j=0}^{N-1} \mathrm{Tr}[\varrho_k \Pi_j] \log_2 \left\{ \frac{\mathrm{Tr}[\varrho_k \Pi_j]}{N^{-1} \sum_{h=0}^{N-1} \mathrm{Tr}[\varrho_h \Pi_j]} \right\}. \tag{10}$$

By using again the covariance property of the POVM and its explicit form given in Eq. (6), the conditional probability can be expressed as

$$\begin{aligned} p(j|k) &= \mathrm{Tr}[\rho_k \Pi_j] = \mathrm{Tr}[\rho_0 \Pi_{j-k}] \\ &= \sum_{n,m=0}^{\infty} A_{n,m} f_{n-m}(j-k) \rho_{n,m}. \end{aligned} \tag{11}$$

Note that $\sum_k p(j|k) = \sum_k \mathrm{Tr}[\rho_k \Pi_j] = 1$, which follows from the symmetries of the resolution function, $f_{-d}(j) = f_d(j)$; i.e., $f_{-d}(-j) = f_d(j)$. Upon introducing the positive quantity $s = |j-k|$, we obtain a simpler form for the mutual information

$$I \equiv I(N,\bar{n}) = \log_2 N + \sum_{s=0}^{N-1} q(s) \log_2 q(s), \tag{12}$$

where $\bar{n}$ is the average number of photons of the seed signal and

$$q(s) = \sum_{n,m=0}^{\infty} A_{n,m} f_{n-m}(s) \rho_{n,m} \tag{13}$$

$$= \frac{1}{N}\left\{1 + \sum_{n=0}^{\infty}\sum_{d=1}^{\infty} A_{n,n+d}[f_d(s)\rho_{n,n+d} + \text{c.c.}]\right\}. \tag{14}$$

The function $q(s)$ measures the probability of finding a $2\pi s/N$ phase difference between the input and output signal, whatsoever value the encoded phase may assume.

The function $q(s)$ and thus the performances of the communication channel do depend on the measurement performed by the receiver through the matrix $(A_{n,m})$ and on the seed state via the matrix elements $\rho_{n,m} = \langle n|\rho_0|m\rangle$. In the following, we will focus on two particular phase measurements: the canonical phase measurement [11–15] and a phase-space-based one, i.e., the marginal phase distribution obtained from the Husimi Q function [16–25]. The latter is a feasible phase measurement achievable, e.g., by heterodyne or double-homodyne detection. For the canonical measurement we have $A_{n,m} = 1$, whereas for the Q measurement $A_{n,m} = \Gamma[1 + \frac{1}{2}(n+m)](n!m!)^{-\frac{1}{2}}$, $\Gamma[x]$ being the Euler Gamma function.

III. QUANTUM PHASE COMMUNICATION CHANNELS IN THE PRESENCE OF STATIC PHASE DIFFUSION

In this section we address quantum phase communication channels in the presence of phase diffusion, and start by considering situations where the environmental noise is static. Any phase communication channel is based on the observation that the optical field produced by a laser provides a convenient quantum system for carrying information. In particular, coherence of laser source ensures that a well-defined phase can be attributed to a light mode. Still, the unavoidable presence of noise generates a phase diffusion, which ultimately limits the coherence of the light. The master equation governing the evolution of the light beam in a static phase diffusing environment may be written as [10,26]

$$\frac{d}{dt}\rho = \frac{\Gamma}{2}\mathcal{L}[a^\dagger a]\rho, \tag{15}$$

where $\mathcal{L}[O]\rho = 2O\rho O^\dagger - O^\dagger O\rho - \rho O^\dagger O$ and Γ is the static phase noise factor. An initial state $\rho(0)$ evolves with time as

$$\rho(t) = \sum_{n,m=0}^{\infty} e^{-\frac{1}{2}\tau(n-m)^2}\rho_{n,m}|n\rangle\langle m|, \tag{16}$$

where we introduced the rescale time $\tau = \Gamma t$. One can easily see that the diagonal elements $\rho_{n,n}$ are unaffected by the phase noise; thus, energy is conserved, whereas the off-diagonal elements decay away exponentially.

In the rest of our paper we assume that the input seed is a coherent state of the radiation field; namely, $\rho_0 = |\alpha\rangle\langle\alpha|$, with

$$|\alpha\rangle = e^{-|\alpha|^2/2}\sum_{n=0}^{\infty}\frac{\alpha^n}{\sqrt{n!}}|n\rangle. \tag{17}$$

Without lack of generality, we assume α to be real. The density matrix elements associated with the initial coherent state ρ_0 are

$$\rho_{n,m} = e^{-\bar{n}}\frac{\bar{n}^{(n+m)/2}}{\sqrt{n!m!}}, \tag{18}$$

where $\bar{n} \equiv \alpha^2$ is the average number of photons of the coherent state ρ_0. Exploiting Eq. (16), we find that the state arriving at the receiver after the propagation through the noisy channel has the following density matrix elements:

$$\rho_{n,m} \to \rho_{n,m}(t) = e^{-\frac{1}{2}\tau(n-m)^2}\rho_{n,m}, \tag{19}$$

which can be used to evaluate the mutual information as written in Eq. (12) once the POVM describing the measurement is given and, thus, the $f_{n-m}(s)$ are assigned.

The POVM describing the ideal (canonical) measurement is obtained from Eq. (4) with $A_{n,m} = 1$, $\forall n,m$. In turn, the probability $q(s)$ after the phase diffusion process reads

$$q_c(s) = \frac{1}{N}\left\{1 + 2e^{-\bar{n}}\sum_{n=0}^{\infty}\sum_{d=1}^{\infty}\text{sinc}\left(\frac{\pi d}{N}\right)e^{-\frac{1}{2}d^2\tau} \times \cos\left[\frac{\pi d}{N}(2s+1)\right]\frac{\bar{n}^{n+d/2}}{\sqrt{n!(n+d)!}}\right\}, \tag{20}$$

where $\text{sinc}(x) = \sin(x)/x$. The channel capacity with ideal receivers is given by the mutual information I_c that directly follows from Eq. (12).

The probability $q_Q(s)$ for the Q-measurement process is obtained using $A_{n,m} = \Gamma[1 + \frac{1}{2}(n+m)](n!m!)^{-\frac{1}{2}}$:

$$q_Q(s) = \frac{1}{N}\left\{1 + 2e^{-\bar{n}}\sum_{n=0}^{\infty}\sum_{d=1}^{\infty}\text{sinc}\left(\frac{\pi d}{N}\right)e^{-\frac{1}{2}d^2\tau} \times \cos\left[\frac{\pi d}{N}(2s+1)\right]\frac{\Gamma\left(1+n+\frac{d}{2}\right)\bar{n}^{n+d/2}}{n!(n+d)!}\right\}. \tag{21}$$

The corresponding channel capacity I_Q is again obtained using Eq. (12).

In the upper panels of Fig. 2 we show the channel capacity as a function of the rescaled time variable τ, which plays the role of a noise parameter, for ideal (upper left panel) and Q (upper right panel) phase receivers and for different values $\bar{n}$ of the average number of photons of the seed state. The size of the alphabet is set to $N = 20$. As is apparent from the plots, phase diffusion leads to an unavoidable loss of information. The mutual information I_Q for Q receivers shows the same vanishing behavior in time as the ideal one I_C, though its value is always slightly smaller. In order to provide a quantitative assessment we show their ratio I_Q/I_c in the lower panel of the same figure, as a function of τ for different values of $\bar{n}$. The ratio is always below 1, thus confirming that Q receivers are not as efficient as the ideal ones. The ratio slightly increases with time, i.e., for long-distance channels, and with the energy of the seed signal.

In order to further assess the performances of phase channels we now compare the mutual information I_c and I_Q with the capacity of a (realistic) coherent channel and with the ultimate quantum capacity of a single-mode channel, which is achieved by the photon number channel. In a coherent channel information is encoded onto the amplitude

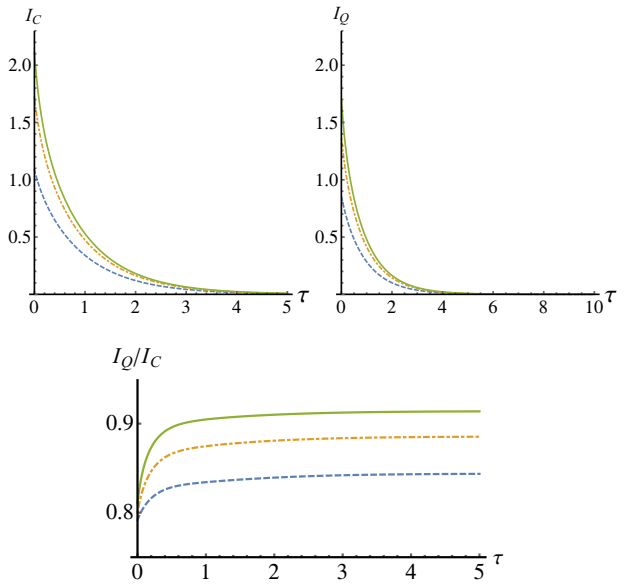

FIG. 2. (Color online) Phase communication channels in the presence of static phase diffusion. The upper panels show the capacities for the ideal receiver I_C (left) and the Q one I_Q (right) as a function of the noise parameter $\tau = \Gamma t$ for different values of the average number of photons: from bottom to top, $\bar{n} = 1$ (dashed blue), $\bar{n} = 2$ (dot-dashed orange), $\bar{n} = 3$ (solid green). We set the alphabet size to $N = 20$. The lower panel shows the ratio I_Q/I_C as a function of τ for different values of the average number of photons: from bottom to top, $\bar{n} = 1$ (dashed blue), $\bar{n} = 2$ (dot-dashed orange), $\bar{n} = 3$ (solid green).

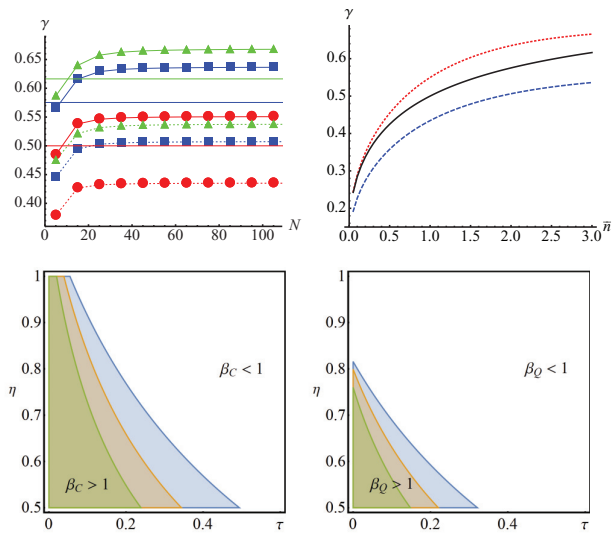

FIG. 3. (Color online) The upper left panel shows the ratios γ_C (symbols joined by solid lines) and γ_Q (symbols joined by dotted lines) as a function of the number of symbols in the alphabet for noiseless phase channels ($\eta = 1$). Red circles correspond to $\bar{n} = 1$, blue squares to $\bar{n} = 2$, and green triangles to $\bar{n} = 3$. Solid lines are the ratios $C_{\rm COH}/C_{\rm PHN}$ for the same three values of $\bar{n}$ (from bottom to top) with the same color code. The upper right panel shows the ratios γ_C (dotted red), $C_{\rm COH}/C_{\rm PHN}$ (solid black), and γ_Q (dashed blue) for noiseless channels as a function of $\bar{n}$ and for a fixed value of $N = 50$. The lower panels show the regions $\beta_C > 1$ and $\beta_Q > 1$, respectively, as functions of $\tau = \Gamma t$ and η. From left to right we have the regions corresponding to $\bar{n} = 1,2,3$ (green, orange, and blue, respectively). When $\beta_k > 1$, $k = C, Q$, the phase channels become more effective than coherent ones. The boundary of each region singles out an energy-dependent threshold on the noise parameters.

of a coherent signal and then retrieved by heterodyne or double-homodyne detectors; the channel capacity is achieved by Gaussian modulation of the amplitude and is given by

$$C_{\rm COH}(\eta) = \log_2(1 + \eta\bar{n}), \tag{22}$$

where $\bar{n}$ is again the average number of photon per use of the channel, and η is the overall (amplitude) loss along the channel. On the other hand, the ultimate quantum capacity of a single-mode channel, which also saturates the Holevo-Ozawa-Yuen bound [1], is achieved by the photon number channel

$$C_{\rm PHN} = (\bar{n} + 1)\log_2(\bar{n} + 1) - \bar{n}\log_2\bar{n}, \tag{23}$$

where information is encoded onto the number of quanta transmitted through the channel according to a thermal distribution, and the decoding stage is performed by photodetection.

At first, let us address noiseless phase channels and consider, for both receivers, the ratio between the corresponding mutual information and the ultimate capacity, i.e., $\gamma_C = I_C/C_{\rm PHN}$ and $\gamma_Q = I_Q/C_{\rm PHN}$. The two quantities are reported in the upper left panel of Fig. 3 as a function of the number of symbols in the phase alphabet, and for different values of the average number of photons $\bar{n}$. The plots reveal that an alphabet of about $N \simeq 50$ symbols is enough to reach the asymptotic value of both ratios, and in turn of I_C and I_Q. Also, the plots show that the ratio with the ultimate capacity is comparable to that of noiseless coherent channels, with ideal phase receivers slightly outperforming the coherent channel and the Q one being slightly outperformed. Using this size of the alphabet, we have evaluated γ_C and γ_Q as a function of the average photon number $\bar{n}$. Results are shown in the upper right panel of Fig. 3, confirming that phase channels with ideal receivers perform slightly better than coherent ones, whereas Q receivers lead to slightly worse performances.

Let us now compare phase channels with coherent ones in the presence of noise. In the lower panels of Fig. 3 we show the ratios $\beta_k = I_k/C_{\rm COH}$, $k = C, Q$, between the capacity of the phase channels and the capacity of the coherent channel as a function of the noise parameters, τ and η, of the two channels. Results for different values of the average number of photons $\bar{n}$ are shown. In both cases an energy-dependent threshold on the amount of noise appears, above which phase channels become more effective than coherent ones. In particular, we notice that noisy phase channels with ideal receivers may outperform ideal coherent channels, while this phenomenon is absent when using the Q receivers.

Finally, let us discuss the performances of the two receivers in the relevant quantum regime of low number of photons, $\bar{n} \ll 1$, and large number of letters, $N \gg 1$. As can be argued from the upper right of Fig. 3, both I_C and I_Q grow linearly with $\bar{n}$ for $\bar{n} \ll 1$, and this resembles the behaviour of both the coherent capacity and the ultimate quantum capacity. This

means that, albeit being suboptimal, phase channels offer good performances when low energy should be transmitted through the channel. This finding can be confirmed by expanding the channel capacity up to the first order in the average photon number of the seed signal, arriving at the expressions

$$I_{\rm ID} \overset{\bar{n}\ll 1}{\simeq} \frac{\bar{n}\,\mathrm{sinc}^2\left(\frac{\pi}{N}\right)e^{-\tau}}{\log_{10}2} \overset{N\gg 1}{\simeq} \frac{\bar{n}\,e^{-\tau}}{\log_{10}2} \tag{24}$$

for the ideal measurement and

$$I_{\rm Q} \overset{\bar{n}\ll 1}{\simeq} \frac{\pi}{4}\frac{\bar{n}\,\mathrm{sinc}^2\left(\frac{\pi}{N}\right)e^{-\tau}}{\log_{10}2} \overset{N\gg 1}{\simeq} \frac{\pi}{4}\frac{\bar{n}\,e^{-\tau}}{\log_{10}2} \tag{25}$$

for the Q-receiver one, their ratio approaching the limiting value of $\pi/4$.

IV. DYNAMICAL PHASE DIFFUSION

In many experimental situations, the exchange of information between sender and receiver takes place in noisy environments which cannot be described in terms of a Markovian master equation. In such cases, a full quantum description of the interaction may be inconvenient, as the approximations needed to obtain solvable dynamical equations could preclude the study of interesting features of the dynamics itself. On the other hand, when the exact quantum description is not achievable, it is still possible to model the interaction by classical stochastic fields (CSFs), which happen to be reliable models of quantum environments, especially when the noise presents classical features, e.g., a Gaussian noise [27–30]. Moreover, the use of a CSF also gives the chance to analyze in a simple way the role of the correlation time of the environment, and the influence on the dynamics of the presence of a detuning between the mode playing the role of information carrier and the central (natural) frequency of the environment.

In the following, we consider a generalized phase diffusion model corresponding to the quantum map

$$\rho(\tau) = \int_{-\infty}^{\infty} \frac{d\phi}{\sqrt{2\pi\sigma(\tau)}}\, e^{-\frac{\phi^2}{2\sigma(\tau)}}\, U(\phi)\rho(0)U^{\dagger}(\phi), \tag{26}$$

where $\sigma(\tau)$ is a time-dependent variance, summarizing the dynamical properties of the environment, and, for convenience, we still use the rescaled time $\tau = \Gamma t$. The static environment of the previous section is recovered for $\sigma(\tau) = \tau$. The quantum map (26) turns the input state ρ_k into a statistical mixture of states with a time-dependent Gaussian distribution of the phase around the original phase ϕ_k. The time dependence of $\sigma(\tau)$ is linked to the correlation function of the underlying stochastic noise as follows:

$$\sigma(\tau) = \int_0^t ds_1 \int_0^t ds_2 \cos[\delta(s_1 - s_2)]\, K(s_1, s_2), \tag{27}$$

where $K(s_1,s_2)$ is the correlation function of the specific CSF chosen to describe the noise and $\delta = (\omega_0 - \omega)/\Gamma$ is the rescaled detuning between the carrier frequency ω_0 and the central frequency of the environmental spectrum ω. In this paper, we focus on the noise generated by the Ornstein-Uhlenbeck process with a Lorentzian spectrum and correlation function $K(\tau_1,\tau_2) = \frac{1}{2}\lambda\,\tau_E^{-1}\,\exp(-|\tau_1 - \tau_2|/\tau_E)$, where τ_E is the characteristic time of the environment and λ is the dynamical phase noise factor, rescaled with Γ. In this case, $\sigma(\tau)$ is given by

$$\sigma(\tau) = \frac{\lambda}{[1+(\delta\,\tau_E)^2]^2}(\tau - \tau_E + (\delta\,\tau_E)^2(\tau + \tau_E) + \tau_E\, e^{-\tau/\tau_E}\{[1-(\delta\,\tau_E)^2]\cos\delta\,\tau - 2\delta\,\tau_E \sin\delta\,\tau\}). \tag{28}$$

In the Markovian limit $\tau_E \ll \tau$, the latter may be rewritten as

$$\sigma(\tau) \simeq \lambda\tau \tag{29}$$

whereas, in the presence of highly correlated environments $\tau_E \gg \tau$, it becomes

$$\sigma(\tau) \simeq \tfrac{1}{2}\lambda\tau^2/\tau_E. \tag{30}$$

Equation (29) confirms that the quantum map (26) is the solution of the Markovian master equation for a static phase-diffusing environment, upon setting $\lambda = 1$. In this case the environment is characterized by a very short correlation and the stochastic field describes a Markovian interaction. The corresponding dynamics of mutual information approaches that illustrated in Fig. 2.

If the environment shows nonzero correlation time the dynamics of mutual information may be dramatically altered, showing either a different decay rate or the appearance of oscillations. In the following we first analyze the case of a *resonant environment* with zero detuning $\delta = 0$ and then focus attention on nonresonant situations. In both cases, the probabilities $q_k(s)$, $k = C, Q$ are still given by Eqs. (20) and

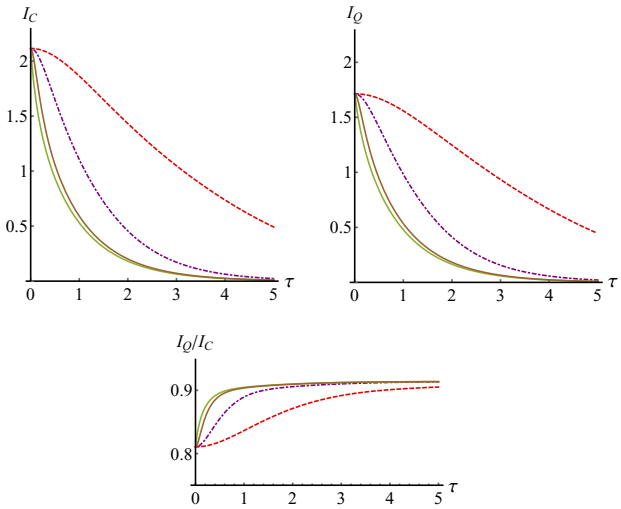

FIG. 4. (Color online) Phase communication channels in the presence of dynamical phase diffusion. The upper panels show the mutual information I_C (left) and I_Q (right) as functions of $\tau = \Gamma t$ for different values of the correlation time τ_E of the environment. From bottom to top, $\tau_E = 0.1$ (solid brown), 1 (dot-dashed purple), 10 (dashed red). The lower solid green curve is the mutual information in the static case. The other parameters read as follows: $N = 20$, $\lambda = 1$, $\bar{n} = 3$. The lower panel shows the ratio I_Q/I_C as a function of τ for the same values of τ_E and of the other parameters. The color code is the same as in the upper panels.

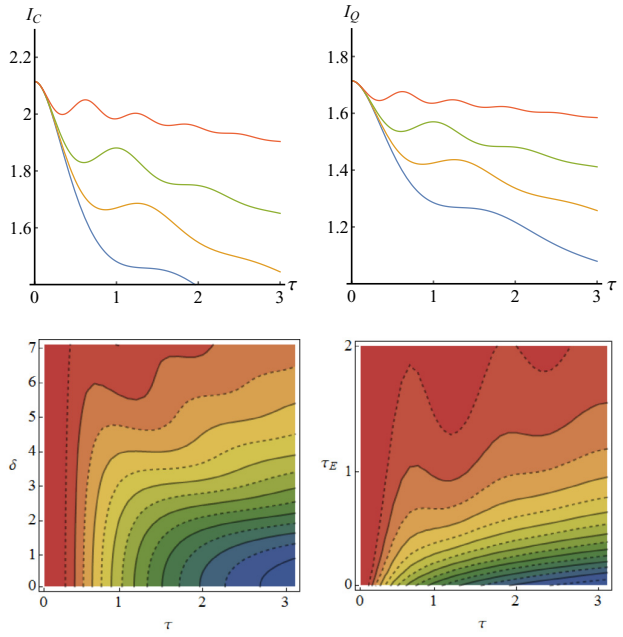

FIG. 5. (Color online) Phase communication channels in the presence of dynamical phase diffusion. The upper panels show the channel capacities (or mutual information) I_C (left) and I_Q (right) as a function of $\tau = \Gamma t$ for different values of detuning. From top to bottom $\delta = 10$ (red), $\delta = 6$ (green), $\delta = 4.5$ (orange), and $\delta = 3.5$ (blue). The other parameters are given by $N = 20$, $\lambda = 1, \bar{n} = 3, \tau_E = 1$. The lower left panel shows the contour plots of I_C as a function of τ and detuning δ for $N = 20$, $\lambda = 1$, $\bar{n} = 3$, and $t_E = 1$. The right panel contains the contour plots I_Q as a function of τ and t_E for $N = 20$, $\lambda = 1$, $\bar{n} = 3$, and $\delta = 5.5$.

(21) with the replacement

$$\exp\left(-\tfrac{1}{2}d^2\tau\right) \longrightarrow \exp\left[-\tfrac{1}{2}d^2\sigma(\tau)\right].$$

Let us start with the case of a resonant environment ($\delta = 0$). Under such condition, $\sigma(t)$ reduces to

$$\sigma(\tau) = \lambda[\tau - \tau_E(1 - e^{-\tau/\tau_E})] \tag{31}$$

and the channel appears to be more robust against the effects of noise, at least for a short-time dynamics, compared to the static case. In order to illustrate this feature, in Fig. 4, we show the mutual information I_C and I_Q as a function of τ for different values of τ_E. As is apparent from the plot, the presence of a nonzero correlation time of the environment τ_E better preserves the capacity against phase diffusion for both ideal and Q receiver. As happens in the static case the mutual information vanishes with time. However, a time-correlated environment allows a "concave dynamics" of the mutual information, which lasts longer, the higher is the correlation time. This behavior is due to the transition from linear to quadratic behavior of $\sigma(\tau)$, see Eq. (30), which may be observed for increasing τ_E. We also show the capacity for the static case (solid green line) for comparison. In the lower panel of the same figure we report the ratio I_Q/I_C as a function of τ. Upon comparing this plot with the lower panel of Fig. 2 we conclude that dynamical noise is more detrimental for Q receivers than for ideal ones.

Let us now analyze the effects of detuning between the frequency of the information carrier and the central frequency of the CSF. As it is possible to see from the upper panels of Fig. 5, the dynamics of the capacity is strongly affected by the detuning for both kind of receivers. On the one hand, the detuning contributes to the significative slowdown of the damping of mutual information and, on the other hand, it is responsible for the appearance of revivals of capacity, which can be interpreted as a sign of a backflow of information caused by the non-Markovian effect of the detuned dynamical map. Yet, the contour plots of mutual information, shown in the lower panels of the same figure, reveal that the presence of revivals is also related to the correlation time of the environment. In the left panel, we show that for fixed correlation time of the environment $\tau_E = 1$ revivals appear only for particular values of detuning δ. In the right panel, we show that for fixed value of detuning $\delta = 5.5$ revivals appear beyond a threshold value of the correlation time of the environment.

V. CONCLUSIONS

We have analyzed quantum phase communication channels based on phase modulation of coherent states and addressed their performances in the presence of static and dynamical phase diffusion by evaluating the channel capacity for ideal and realistic phase receivers. In terms of performance, our results show that phase communication channels are robust, especially for large alphabets in the low-energy regime, and that their performances are comparable to those of coherent channels in the presence of loss.

In the presence of dynamical (non-Markovian) phase diffusion, phase channels become more robust, the channel capacity being preserved by the time correlations of the environment. When the noise spectrum is detuned with respect to the information carrier, revivals of capacity also appear.

Our results illustrate the potential applications of phase-keyed M-ary channels and may be also of interest in other schemes where the information is coded on phase shifts as, for example, in interferometric high-sensitivity measurements.

ACKNOWLEDGMENTS

This work was supported by MIUR through the FIRB project "LiCHIS" (Grant No. RBFR10YQ3H), by EU through the Collaborative Projects and QuProCS (Grant Agreement No. 641277), and by UniMI through H2020 Transition Grant No. 14-6-3008000-625.

[1] H. P. Yuen and M. Ozawa, Phys. Rev. Lett. **70**, 363 (1993).
[2] C. M. Caves and P. D. Drummond, Rev. Mod. Phys. **66**, 481 (1994).
[3] A. S. Holevo and R. F. Werner, Phys. Rev. A **63**, 032312 (2001).
[4] V. Giovannetti, S. Guha, S. Lloyd, L. Maccone, J. H. Shapiro, and H. P. Yuen, Phys. Rev. Lett. **92**, 027902 (2004).

[5] J. Shapiro, S. Guha, and B. Erkmen, J. Opt. Networking **4**, 501 (2005).
[6] S. E. Fedorov and A. N. Mart'yanov, Radio Eng. Electr. Phys. **26**, 36 (1981).
[7] G. M. D'Ariano, C. Macchiavello, N. Sterpi, and H. P. Yuen, Phys. Rev. A **54**, 4712 (1996).
[8] M. J. W. Hall, J. Mod. Opt. **40**, 809 (1993).
[9] S. Olivares, S. Cialdi, F. Castelli, and M. G. A. Paris, Phys. Rev. A **87**, 050303(R) (2013).
[10] M. G. Genoni, S. Olivares, and M. G. A. Paris, Phys. Rev. Lett. **106**, 153603 (2011).
[11] R. Lynch, Phys. Rep. **256**, 367 (1995).
[12] U. Leonhardt, J. A. Vaccaro, B. Böhmer, and H. Paul, Phys. Rev. A **51**, 84 (1995).
[13] M. G. A. Paris, Nuovo Cim. B **111**, 1151 (1996); Fizika. B **6**, 63 (1997).
[14] A. Royer, Phys. Rev. A **53**, 70 (1996).
[15] M. G. A. Paris, Phys. Rev. A **60**, 5136 (1999).
[16] J. W. Noh, A. Fougeres, and L. Mandel, Phys. Rev. Lett. **67**, 1426 (1991); Phys. Rev. A **45**, 424 (1992); **46**, 2840 (1992).
[17] Z. Hradil, Phys. Rev. A **47**, 4532 (1993).
[18] J. W. Noh, A. Fougeres, and L. Mandel, Phys. Rev. A **47**, 4535 (1993).
[19] M. Freiberger, W. Vogel, and W. Schleich, Phys. Lett. A **176**, 41 (1993).
[20] G. M. D'Ariano and M. G. A. Paris, Phys. Rev. A **48**, R4039 (1993).
[21] U. Leonhardt and H. Paul, Phys. Rev. A **48**, 4598 (1993).
[22] G. M. D'Ariano and M. G. A. Paris, Phys. Rev. A **49**, 3022 (1994).
[23] P. Busch, M. Grabowski, and P. J. Lahti, *Operational Quantum Physics*, Lecture Notes in Physics, Vol. 31 (Springer, Berlin, 1995).
[24] H. Wiseman, Phys. Rev. Lett. **75**, 4587 (1995).
[25] J.-P. Pellonpää, J. Schultz, and M. G. A. Paris, Phys. Rev. A **83**, 043818 (2011).
[26] M. G. Genoni, S. Olivares, D. Brivio, S. Cialdi, D. Cipriani, A. Santamato, S. Vezzoli, and M. G. A. Paris, Phys. Rev. A **85**, 043817 (2012).
[27] D. Crow and R. Joynt, Phys. Rev. A **89**, 042123 (2014).
[28] C. Benedetti, M. G. A. Paris, and S. Maniscalco, Phys. Rev. A **89**, 012114 (2014).
[29] J. Trapani, M. Bina, S. Maniscalco, and M. G. A. Paris, Phys. Rev. A **91**, 022113 (2015).
[30] G. M. D'Ariano, C. Macchiavello, and M. G. A. Paris, in *Quantum Communication and Measurement*, edited by V. P. Belavkin, O. Hirota, and R. L. Hudson (Plenum Press, New York, 1995), pp. 339–350.